Effective Stiffening and Damping Enhancement of Structures With Strongly Nonlinear Local Attachments

Themistoklis P. Sapsis
Department of Mechanical Engineering,
Massachusetts Institute of Technology,
Cambridge, MA 02139
e-mail: sapsis@mit.edu

D. Dane Quinn
Department of Mechanical Engineering,
The University of Akron,
Akron, OH 44325
e-mail: quinn@uakron.edu

Alexander F. Vakakis
Department of Mechanical Science and Engineering,
University of Illinois at Urbana-Champaign,
Urbana, IL 61801
e-mail: avakakis@illinois.edu

Lawrence A. Bergman
Department of Aerospace Engineering,
University of Illinois at Urbana-Champaign,
Urbana, IL 61801
e-mail: lbergman@illinois.edu

We study the stiffening and damping effects that local essentially nonlinear attachments can have on the dynamics of a primary linear structure. These local attachments can be designed to act as nonlinear energy sinks (NESs) of shock-induced energy by engaging in isolated resonance captures or resonance capture cascades with structural modes. After the introduction of the NESs, the effective stiffness and damping properties of the structure are characterized through appropriate measures, developed within this work, which are based on the energy contained within the modes of the primary structure. Three types of NESs are introduced in this work, and their effects on the stiffness and damping properties of the linear structure are studied via (local) instantaneous and (global) weighted-averaged effective stiffness and damping measures. Three different applications are considered and show that these attachments can drastically increase the effective damping properties of a two-degrees-of-freedom system and, to a lesser degree, the stiffening properties as well. An interesting finding reported herein is that the essentially nonlinear attachments can introduce significant nonlinear coupling between distinct structural modes, thus paving the way for nonlinear energy redistribution between structural modes. This feature, coupled with the well-established capacity of NESs to passively absorb and locally dissipate shock energy, can be used to create effective passive mitigation designs of structures under impulsive loads. [DOI: 10.1115/1.4005005]

Keywords: nonlinear stiffening, nonlinear damping enhancement, nonlinear energy sink

1 Introduction

It is well established that stiffness nonlinearity can lead to hardening (or softening) effects in the dynamics of mechanical oscillators [1]. This effect is evidenced by an increase (or decrease) in the frequency of oscillation of a system with increasing energy, and in weakly nonlinear systems it can be analytically studied by applying qualitative and quantitative methodologies. Indeed, most studies in the current literature consider weakly nonlinear stiffening effects in structures possessing nonlinear (but linearizable) stiffness or damping elements (e.g., weakly nonlinear springs) [1]. Manevitch extended this analysis to strongly nonlinear (i.e., nonlinearizable) mechanical oscillators through a complexification/averaging approach [2]. In additional works, stiffening effects in material systems, biophysical, and biomedical applications have been investigated. Aboudi [3] studied the combined nonlinear effects of stiffening fibers in a softening resin matrix on the overall behavior of graphite/epoxy composites following a micromechanical approach. In biophysics-related studies, Karray et al. [4] proposed a control procedure for the active stiffening motion of a class of flexible structures with nonlinear affine dynamics. Xu and Kup [22] studied stress stiffening in models of dendritic actin networks of living cells, and Kasza et al. [5] studied the stiffening of the dynamics of cells under large applied forces.

In a separate series of works, metamaterials with the property of negative stiffness have been considered. Negative stiffness was achieved on a local basis via the incorporation into a matrix material of tailored inclusions that exhibit post-buckled behavior and, thus, negative stiffness over a portion of their load-deformation behavior. According to Lakes [6] and Wang and Lakes [7], as the matrix damping becomes small, the composite damping and stiffness are driven higher, even for a minute concentration of inclusions, exceeding the properties of either the inclusions or matrix materials alone. An additional metamaterial concept providing enhanced performance can be found, for example, in the work of Huang and Sun [8], who employ negative effective mass density in order to achieve wave attenuation.

The enhancement of the damping properties of a (linear) structure and its capacity for enhanced energy dissipation due to nonlinear structural modifications has been less studied, with most current studies focusing on stiffening effects. This work investigates the enhancement of the stiffness and damping properties of a linear structure via structural modification through the addition of strongly nonlinear structural modules that behave, in essence, as nonlinear energy sinks (NESs) [9]. The premise of this work is that properly designed NESs can affect significantly the stiffness and damping properties of the structures to which they are attached by rapidly and passively absorbing and dissipating vibration energy in a one-way process through a series of transient resonance captures [10]. The dynamical mechanism that governs the operation of the NESs is passive targeted energy transfer (TET), and it has been analyzed analytically, numerically, and experimentally [9,11–14]. This is enabled by the absence of linear components in the dynamics of the NESs, so that *local* NESs can induce *global* nonlinear effects in the dynamics of the structures to which they are attached. As discussed in Ref. [9] and the references therein, essentially nonlinear stiffnesses can be reliably reproduced through the geometric nonlinearity of linear stiffness elements. In particular, an elastic wire with no pretension when fixed at its ends and forced by a transverse force reacts in an essentially nonlinear manner [15].

A manifestation of these global effects is the nonlinear stiffening (or softening) of the dynamics of the structure, as well as damping enhancement, as evidenced by the increased rate of the decrease of specific energy norms that is defined in this work. We define quantitative measures characterizing the stiffening and

Contributed by the Technical Committee on Vibration and Sound of ASME for publication in the JOURNAL OF VIBRATION AND ACOUSTICS. Manuscript received December 13, 2010; final manuscript received July 11, 2011; published online January 9, 2012. Assoc. Editor: Philip Bayly.

 Copyright © 2012 by ASME

Downloaded 09 Jan 2012 to 18.7.29.240. Redistribution subject to ASME license or copyright; see http://www.asme.org/terms/Terms_Use.cfm

damping enhancement of a structure with attached NESs, and we demonstrate the efficacy of these measures for different types of essentially nonlinear attachments. Fundamentally, we aim to show that the use of intentional nonlinearity can provide a new paradigm for the stiffness and damping enhancement of a (linear) structure.

2 Effective Measures for Linear Structures With Essentially Nonlinear Attachments

The principal aim of this work is the exploitation of *intentional strong nonlinearities* introduced through strongly nonlinear attachments within a linear structure for the purpose of enhancing its stiffness and drastically enhancing its effective damping. The intentional strong nonlinearities will be implemented via the addition of specially designed structural modules with essential stiffness and/or damping nonlinearities to the structure. These will act, in essence, as passiveNESs, i.e., as broadband absorbers of shock-induced vibrations of the large-scale structure to which they will be attached. This energy absorption is achieved by means of transient (i.e., occurring over finite time windows) nonlinear resonances—transient resonance captures—between the essentially nonlinear NESs and highly energetic modes. This in turn leads toTETs [9] from linear structural modes to the NESs where energy is confined and locally dissipated without "spreading" back to the linear structure. What makes TET possible in the augmented system is the essential nonlinearity of the NESs, which do not possess linear components in their dynamics and thus do not possess preferential resonance frequencies. This means that the capacity of an NES for resonance depends only on the instantaneous frequency and energy of the augmented structure, so the fully passive NES is adaptive in its capacity to engage in transient resonance with either isolated or a series of structural modes at different frequencies and energies, leading to broadband vibration energy absorption that drastically affects the overall stiffness and damping properties of the augmented structure.

In that context, the addition of local NESs can induce global changes to the structural dynamics in two ways: (a) through the generation of new nonlinear modes in the modified structure-NES system that amount to a stiffening of the dynamics [9], and (b) by drastically increasing the effective damping factors of the structural modes due to rapid (fast-scale) TET from the structure to the NESs, where energy is localized and dissipated. In summary, our nonlinear approach aims to drastically enhance the capacity of a linear structure to passively mitigate shock-induced vibrations via the *synergistic stiffening of the structural dynamics and an enhanced capacity to rapidly dissipate vibration energy*.

Three types of essentially nonlinear attachments (NESs) are considered; these are depicted in Fig. 1. A type-I NES [Fig. 1(*a*)] is a single-degree-of-freedom (SDOF) oscillator with essential stiffness nonlinearity of the third degree and linear viscous damping. The force (F)-response ($x, \dot{x}$) characteristic is given approximately by $F = kx^3 + d\dot{x}$ and lacks a linear stiffness component. A type-II NES [Fig. 1(*b*)] is an SDOF oscillator with essential stiffness nonlinearity of the third degree and geometrically nonlinear viscous damping, with the force-response characteristic given by $F = kx^3 + dx^2\dot{x}$ [16,17]; we emphasize that both stiffness and damping nonlinearities in these devices are caused solely by the *geometry and kinematics of the motion*, as all of their structural elements exhibit *linear* behavior. Finally, a type-III NES [Fig. 1(*c*)] possesses two degrees of freedom that are coupled by means of essentially nonlinear stiffnesses of the third degree and linear viscous damping. The rationale for introducing the type-III NES is that, if properly designed, it can broaden the energy and frequency ranges of efficient nonlinear energy absorption from the linear structure [18]. The capacity of these devices to engage in transient resonance captures and resonance capture cascades with different modes of a linear structure and to induce broadband passive TET has been analytically, computationally, and experimentally demonstrated [9].

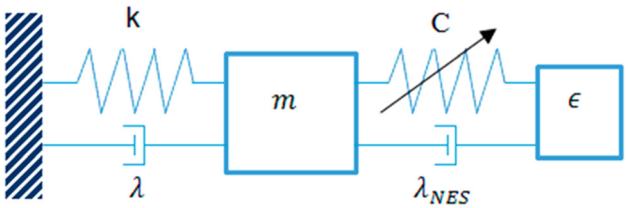

Fig. 2 SDOF linear oscillator with type-I NES attached

The study of the stiffness and damping enhancement of a linear structure due to the addition of a single or multiple NESs requires the formulation of appropriate quantitative measures. These measures should have applicability to linear structures with arbitrarily many degrees of freedom (DOFs) and augmented by an arbitrary number of NESs of different types. In addition, they should be capable of effectively capturing the enhancement of the stiffness and damping of the structure caused by the strongly nonlinear dynamical interactions with the NESs.

We start with the simplest possible case: a linear SDOF oscillator (the structure) coupled to a single type-I NES (Fig. 2). For any specific damped transition, the goal of our analysis is to derive time-dependent effective stiffness and damping coefficients that will allow for the definition of an "effective" linear oscillator capable of reproducing the coupled system. In this way we aim to characterize locally in time the stiffness and damping enhancement of the linear structure due to the presence of the NES. The equations of motion are given as

$$\begin{aligned} m\ddot{q} + \lambda\dot{q} + kq + \lambda_{NES}(\dot{q} - \dot{v}) + C(q - v)^3 &= 0 \\ \varepsilon\ddot{v} + \lambda_{NES}(\dot{v} - \dot{q}) + C(v - q)^3 &= 0 \end{aligned} \tag{1}$$

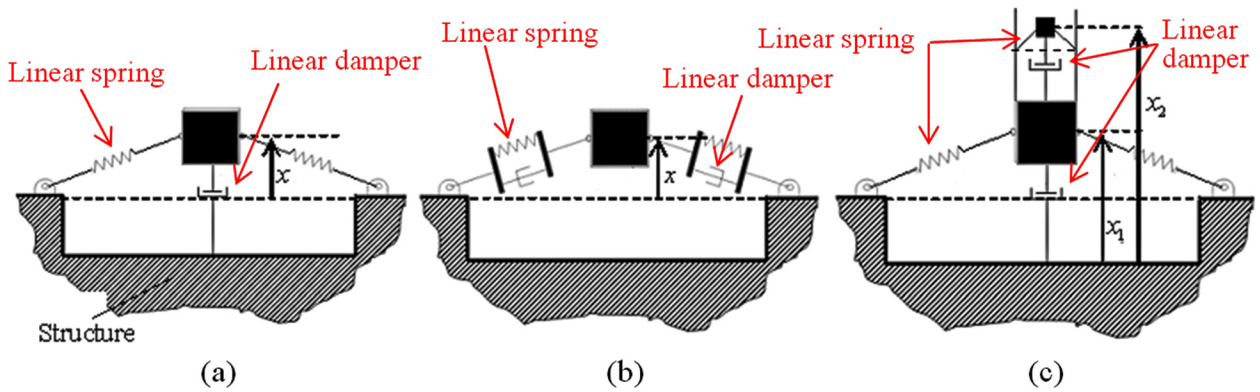

Fig. 1 Essentially nonlinear energy sinks (NESs) considered: (*a*) type-I NES, (*b*) type-II NES, and (*c*) type-III NES. All linear springs and viscous dampers are uncompressed when horizontal.

Downloaded 09 Jan 2012 to 18.7.29.240. Redistribution subject to ASME license or copyright; see http://www.asme.org/terms/Terms_Use.cfm

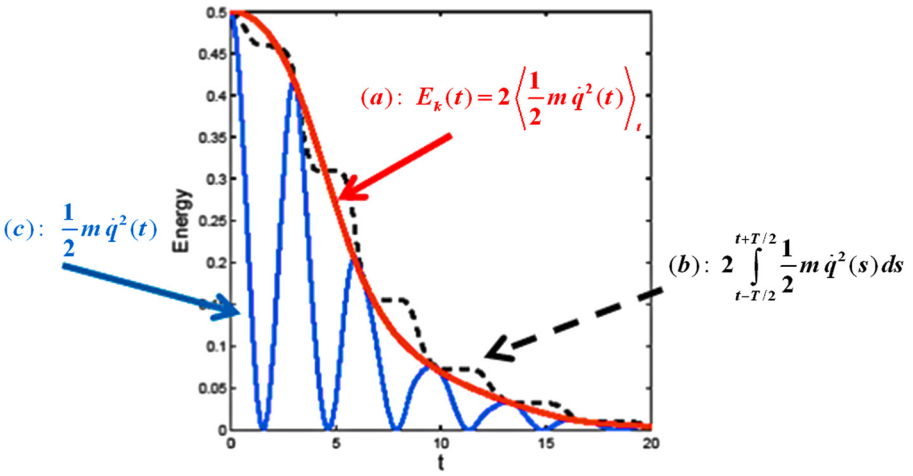

Fig. 3 Averaging of the time series of the kinetic energy of the linear oscillator in Eq. (1). (*a*) Averaged kinetic energy $E_k(t)$ using spline interpolation of local maxima. (*b*) Total mechanical energy in the linear oscillator. (*c*) Instantaneous kinetic energy.

with initial conditions of $\dot{q}(0) = \sqrt{2E_0/m}, q(0) = v(0) = \dot{v}(0) = 0$, where E_0 is the energy induced in the system at $t = 0$. These initial conditions correspond to an impulse applied to the linear oscillator with the system being initially at rest. Our analysis is based on energetic arguments. Specifically, the time-dependent stiffness $k_{eff}(t)$ is computed so that the effective linear oscillator has an instantaneous potential energy that locally in time approximates (in a locally averaged sense) the actual potential energy of the nonlinear system; similarly, the time dependent damping $\lambda_{eff}(t)$ is such that the instantaneous kinetic energy of the effective linear oscillator locally approximates that of the nonlinear system.

Even though the above definitions allow us to obtain effective measures for the stiffness and damping in the system, their practical use is limited, because the instantaneous vanishing of either displacement or velocity leads to singularities in the above measures. In addition, the computation of the potential energy is not always a straightforward process, especially in the case of complex NES configurations or, most important, in experimentally measured responses. To this end, we first need to develop an *averaging process* that can be applied to a time series that is pointwise positive, say, $h^2(t)$. The averaging is performed by constructing a spline interpolation of the local maxima of the time series, denoted by $\langle h^2 \rangle_t$. For the system of Fig. 2, the averaging process is illustrated in Fig. 3, in which the instantaneous kinetic energy computed directly from the velocity time series of the linear oscillator is examined; both the averaged energy $E_k(t)$ as obtained from the spline interpolation and the instantaneous mechanical energy in the oscillator are also depicted. The spline-based averaging scheme also enables the estimation of the time-averaged potential energy of the linear oscillator $E_p(t)$ directly from the time-averaged kinetic energy $E_k(t)$. This property follows from the fact that the spline-based averaging applied to the instantaneous kinetic energy essentially estimates the time-averaged total energy $E_{LO}(t) = 2E_k(t)$ contained in the linear oscillator,

$$E_p(t) = E_k(t) = \frac{1}{2} E_{LO}(t) = \left\langle \frac{1}{2} m \dot{q}^2 \right\rangle_t \tag{2}$$

Note that Hilbert transformation could be used as an alternative to the spline averaging method, although, because its numerical computation is based on the fast Fourier transform, numerical boundary artifacts might be introduced in the initial and final parts of the signal. We emphasize that through the above-described averaging approach we are able to define the effective stiffness and damping measures *without* prior knowledge of the NES configuration attached to the SDOF linear oscillator, because it directly analyzes the measured displacement or velocity time series. Thus, the described methodology is ideal for analyzing experimental responses. Based on the above discussion, we define the time-dependent effective stiffness measure as

$$k_{eff}(t) = \frac{2E_p(t)}{\langle q^2 \rangle_t} = \frac{2\left\langle \frac{1}{2} m \dot{q}^2 \right\rangle_t}{\langle q^2 \rangle_t} \tag{3a}$$

and the time-dependent effective damping measure as

$$\lambda_{eff}(t) = -\frac{\frac{dE_{LO}(t)}{dt}}{\langle \dot{q}^2 \rangle_t} = -\frac{2\frac{d}{dt}\left\langle \frac{1}{2} m \dot{q}^2 \right\rangle_t}{\langle \dot{q}^2 \rangle_t} \tag{3b}$$

These "local" instantaneous measures enable us to study over time the stiffening and dissipative effects of the NES for a given damped transition of the linear structure. However, in many situations (e.g., in optimization studies) it is useful to characterize the overall effect of the NES for an entire damped transition by defining the *global* time-independent effective measures $\overline{k_{eff}}$ and $\overline{\lambda_{eff}}$. To this end, we define time-independent weighted-averaged quantities based on the above-described time-dependent measures. A trivial choice would be to consider the time average of the instantaneous measures; however, this choice would not emphasize the performance characteristics of the NES in the regions where it is most important, i.e., in the initial, highly energetic regime of the damped transition. In order to avoid this issue, we define a *weighted-average* according to the instantaneous square of the displacement (for the stiffness) or velocity (for the damping),

$$\overline{k_{eff}} = \frac{\int_0^\infty k_{eff}(s)\langle q^2 \rangle_s ds}{\int_0^\infty \langle q^2 \rangle_s ds} = \frac{2\int_0^\infty \langle \frac{1}{2} m \dot{q}^2 \rangle_s ds}{\int_0^\infty \langle q^2 \rangle_s ds} \tag{4a}$$

$$\overline{\lambda_{eff}} = \frac{\int_0^\infty \lambda_{eff}(s)\langle \dot{q}^2 \rangle_s ds}{\int_0^\infty \langle \dot{q}^2 \rangle_s ds} = -2\frac{\int_0^\infty \frac{d}{ds}\left\langle \frac{1}{2} m \dot{q}^2 \right\rangle_s ds}{\int_0^\infty \langle \dot{q}^2 \rangle_s ds} = \frac{m\dot{q}^2(0)}{\int_0^\infty \langle \dot{q}^2 \rangle_s ds} \tag{4b}$$

These *weighted-average effective stiffness and damping measures* are time-independent and provide overall characterizations of the stiffness and damping effects of the NES for an entire damped

Downloaded 09 Jan 2012 to 18.7.29.240. Redistribution subject to ASME license or copyright; see http://www.asme.org/terms/Terms_Use.cfm

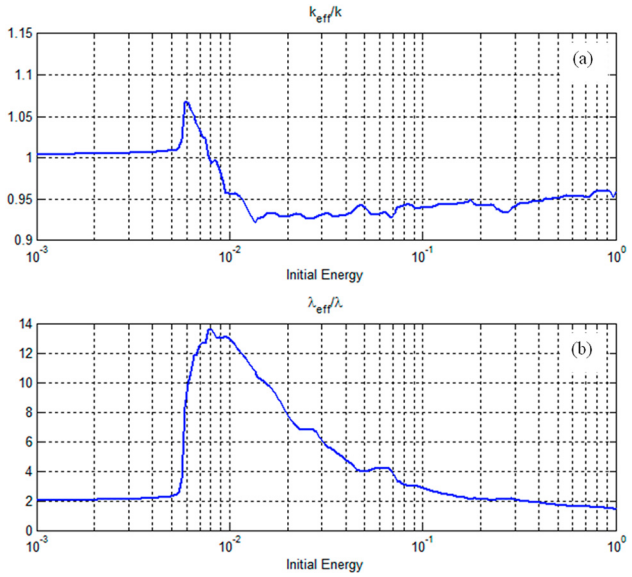

Fig. 4 Weighted-averaged effective measures for varying initial energy E_0 for the impulsively excited system (1): (*a*) $\overline{k_{eff}}/k$, (*b*) $\overline{\lambda_{eff}}/\lambda$

transition of the linear oscillator of system (1). Similar to the corresponding local measures in Eqs. (3*a*) and (3*b*), they are applicable to linear systems with more complex types of NESs attached (i.e., type-II and type-III NESs), and as shown below they can be easily extended to multi-DOF linear primary structures. We emphasize that the descriptions of "local" and "global" in the above-mentioned effective measures refer to the temporal scale of the response, as opposed to the spatial scale of the structure.

As a first demonstration of the application of the global effective measures, in Fig. 4 we depict the variations of $\overline{k_{eff}}$ and $\overline{\lambda_{eff}}$ for linear oscillator system (1) as functions of the initial energy E_0 with the parameters $m = 1, \varepsilon = 0.05, k = 1, \lambda = \lambda_{NES} = 0.005$, and $C = 1$. The significant increase of the weighted-average effective measures above the critical energy threshold $E_0 \approx 5.5 \times 10^{-3}$ is associated with enhanced targeted energy transfer from the directly excited linear oscillator to the type-I NES as discussed in Ref. [9]. We note the significant enhancement of $\overline{\lambda_{eff}}$ to nearly 1400%, compared to the nominal damping value λ immediately after the energy threshold, and the much smaller enhancement of $\overline{k_{eff}}$ in the same energy range; with increasing energy, both measures deteriorate, indicating their sensitivity to energy for the type-I NES. This result shows that the addition of a type-I NES with 5% of the mass of a linear oscillator can increase drastically the effective damping measure when it is excited by impulsive loads in a specific energy range.

In order to demonstrate the local effective measures, we consider two specific damped transitions corresponding to applied impulses with $E_0 = 9 \times 10^{-3}$ (Fig. 5, optimal case) and $E_0 = 0.3$ (Fig. 6, suboptimal case). In Figs. 5(*a*) and 6(*a*) we depict the damped response of the linear oscillator computed by system (1) and compare it to the response of the effective (time-dependent) linear oscillator,

$$m\ddot{q} + \lambda_{eff}(t)\dot{q} + k_{eff}(t)q = 0$$

which takes into account the nonlinear effects induced by the NES through the time-varying instantaneous effective measures $k_{eff}(t)$ and $\lambda_{eff}(t)$. Good correspondence between the exact (simulated) response and the response of the effective oscillator is noted, demonstrating that the previously defined effective measures can successfully capture the effects of the NES in the transient dynamics. In the same plots we depict the response of the damped linear oscillator in Eq. (1) with no NES attached, in order to demonstrate the profound effect that the NES has on the damped dynamics.

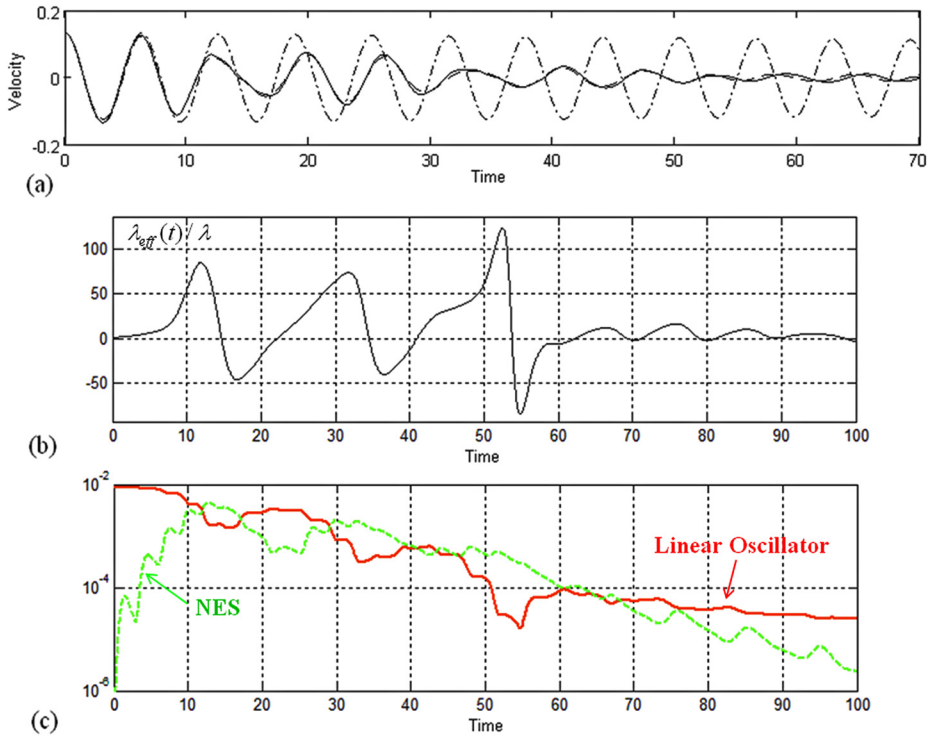

Fig. 5 Damped transition of system (1) for initial energy $E_0 = 9\times10^{-3}$. (*a*) Velocity of the linear oscillator with NES attached (——), of the effective oscillator (- - - -), and of the linear oscillator with no NES attached (-·-·-·-). (*b*) Instantaneous normalized effective damping $\lambda_{eff}(t)/\lambda$. (*c*) Instantaneous energies of the linear oscillator and the NES.

Downloaded 09 Jan 2012 to 18.7.29.240. Redistribution subject to ASME license or copyright; see http://www.asme.org/terms/Terms_Use.cfm

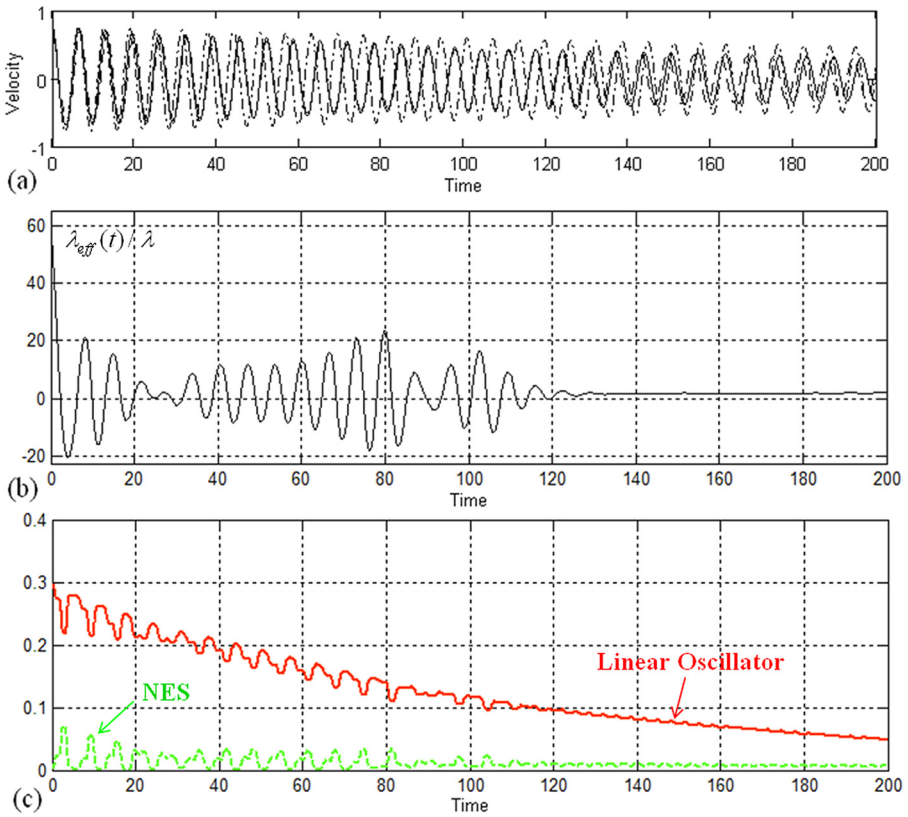

Fig. 6 Damped transition of system (1) for initial energy $E_0 = 0.3$. (*a*) Velocity of the linear oscillator with NES attached (——), of the effective oscillator (- - - -), and of the linear oscillator with no NES attached (·-·-·-·-). (*b*) Instantaneous normalized effective damping $\lambda_{eff}(t)/\lambda$. (*c*) Instantaneous energies of the linear oscillator and the NES.

In Figs. 5(*a*) and 6(*a*) we present the normalized transient effective measure $\lambda_{eff}(t)/\lambda$ for the two energy levels (the effective stiffness measures in both cases are close to unity, so they are not presented). We note that in the optimal case [Fig. 5(*b*)] the normalized effective damping measure attains large positive values in the early, highly energetic regime of the damped dynamics, which explains the high effectiveness of the NES in this case. Lower positive values are noted in the suboptimal case [Fig. 6(*b*)], which explains the lesser performance of the NES for that value of initial energy. In the same plots we note that the instantaneous effective damping assumes *negative* values in certain time intervals. This is explained when we consider the corresponding instantaneous energy exchanges between the linear oscillator and the NES shown in Figs. 5(*c*) and 6(*c*). From these plots we deduce that negative instantaneous effective damping of the linear oscillator occurs over time intervals in which it absorbs energy from the NES through nonlinear beats; this reverse energy exchange is captured by the negative values of effective damping when the NES acts as an energy source.

The previous local and global effective measures can be conveniently extended to multi-DOF linear structures with an arbitrary number of NESs of different types attached to them. This is due to the fact that, as defined, the effective measures are based solely on the response time series of the linear structure, and so modal analysis can be applied toward this aim. To this end, we consider the following undamped and unforced N-DOFs linear system,

$$\underline{M}\,\ddot{\underline{x}} + \underline{K}\,\underline{x} = \underline{0}, \quad \underline{x}(0) = \underline{x}_0, \quad \dot{\underline{x}}(0) = \underline{v}_0 \tag{5}$$

where the underlined capital variables denote matrices and the lowercase bold variables are vectors (and zeros are defined appropriately). In Eq. (5), M and K are $(N \times N)$ matrices and $\underline{x}$ is an N-vector. Assuming that the system has distinct eigenvalues, it admits a modal decomposition from the solution to the eigenvalue problem,

$$\omega_i^2 \underline{M}\,\underline{u}_i = \underline{K}\,\underline{u}_i, \quad i = 1, ..., N \tag{6}$$

where ω_i^2 is the ith natural frequency squared and $\underline{u}_i$ is the corresponding eigenvector. By introducing the coordinate transformation $\underline{x}(t) = \underline{\Phi}\underline{q}(t)$, where $\underline{\Phi}$ is the modal matrix, system (5) is decoupled. Furthermore, assuming that the modal matrix is mass-normalized, it can be expressed as

$$\ddot{\underline{q}}(t) + \underline{\Omega}^2 \underline{q}(t) = \underline{0}, \quad \underline{q}(0) = \underline{\Phi}^T \underline{M}\,\underline{x}_0 \equiv q_0, \quad \dot{\underline{q}}(0) = \underline{\Phi}^T \underline{M}\,\underline{v}_0 \equiv g_0 \tag{7}$$

where $\underline{\Omega}^2$ is the $(N \times N)$ diagonal matrix of natural frequencies squared. Then, the (conserved) total energy E of system (5) can be decomposed in terms of the N modal energies E_i, which are themselves conserved and thus represent invariants of the motion.

$$E = \frac{1}{2}\dot{\underline{q}}^T(t)\dot{\underline{q}}(t) + \frac{1}{2}\underline{q}^T(t)\underline{\Omega}^2\dot{\underline{q}}(t) = \sum_{i=1}^{N} E_i,$$
$$E_i = \frac{1}{2}\dot{\underline{q}}_i^2(t) + \frac{1}{2}\omega_i^2 q_i^2(t) \tag{8}$$

We now consider the N-DOFs linear system with general viscous damping distribution and k NESs attached to it.

Downloaded 09 Jan 2012 to 18.7.29.240. Redistribution subject to ASME license or copyright; see http://www.asme.org/terms/Terms_Use.cfm

$$\underline{M}\,\ddot{\underline{x}} + \underline{C}\,\dot{\underline{x}} + \underline{K}\,\underline{x} = \tilde{\underline{f}}_{NES}(\underline{x},\underline{y}), \quad \underline{x}(0) = \underline{x}_0, \quad \dot{\underline{x}}(0) = \underline{v}_0$$
$$\underline{M}_{NES}\,\ddot{\underline{y}} + \underline{P}_{NES}(\underline{y},\dot{\underline{y}}) = -\underline{f}_{NES}(\underline{x},\underline{y}), \quad \underline{y}(0) = \underline{y}_0, \quad \dot{\underline{y}}(0) = \underline{w}_0 \tag{9}$$

where $\tilde{\underline{f}}_{NES}(\underline{x},\underline{y})$ and $\underline{f}_{NES}(\underline{x},\underline{y})$ represent the N- and k-vectors, respectively, of the nonlinear interaction forces between the linear structure and the attached NESs, and $\underline{y}$ is the k-vector of internal variables describing the motion of the k NESs. Introducing again the modal transformation $\underline{x}(t) = \underline{\Phi}\,\underline{q}(t)$, the N equations of motion of the linear structure can be expressed as

$$\ddot{\underline{q}}(t) + \hat{\underline{C}}\dot{\underline{q}}(t) + \underline{\Omega}^2\underline{q}(t) = \underline{G}_{NES}(\underline{q},\underline{y}), \quad \underline{q}(0) = \underline{\Phi}^T\underline{M}\,\underline{x}_0 \equiv q_0$$
$$\dot{\underline{q}}(0) = \underline{\Phi}^T\underline{M}\,\underline{v}_0 \equiv g_0 \tag{10}$$

where $\hat{\underline{C}} = \underline{\Phi}^T\underline{C}\,\underline{\Phi}$ and $\underline{G}_{NES}(\underline{q},\underline{y}) = \underline{\Phi}^T\tilde{\underline{f}}_{NES}(\underline{\Phi q},\underline{y})$. We note that due to their essential nonlinearities, the NESs now couple each of the linear structural modes, allowing not only for *passive energy absorption and dissipation* (as in the previously discussed SDOF case), but also for *passive modal energy redistribution within the linear structure itself*. This latter effect can have significant beneficial effects in shock mitigation designs, because scattering shock energy from low- to high-frequency structural modes can significantly reduce the amplitude of vibration of the linear structure (in general, higher frequencies are associated with lower amplitudes). In addition, it is well established that higher modes more effectively dissipate vibration energy through structural damping. Such high-frequency scattering has already been reported in seismic mitigation designs based on vibro-impact NESs [19,20].

We define again the (now nonconserved) total energy of the system $E(t)$,

$$E(t) = \frac{1}{2}\dot{\underline{q}}^T(t)\dot{\underline{q}}(t) + \frac{1}{2}\dot{\underline{q}}^T(t)\underline{\Omega}^2\dot{\underline{q}}(t) = \sum_{i=1}^{N} E_i(t)$$
$$E_i(t) = \frac{1}{2}\dot{\underline{q}}_i^2(t) + \frac{1}{2}\omega_i^2 q_i^2(t) \tag{11}$$

We note that again we can express it as a superposition of N modal energies $E_i(t)$; in this case, however, the modal energies are not conserved, because each mode is damped and interacts with the essentially nonlinear NESs, and also with the other modes (with modal coupling provided by the essential nonlinearities of the attached NESs). However, because each of the linear modes represents an SDOF linear oscillator coupled to the NESs, and because the local and global effective measures defined previously rely only on the response time series of the linear structure (with the effects of the attached NESs being implicitly accounted for, only through the variations of the instantaneous modal energies), we can employ the definitions in Eqs. (3*a*), (3*b*), (4*a*), and (4*b*) to define effective stiffness and damping modal measures for system (9).

In order to provide an example of nonlinear coupling between linear structural modes due to the action of an essentially nonlinear NES, we consider the transient dynamics of a two-DOFs damped linear oscillator with a type-I NES attached to it, for impulsive excitation of its lower frequency mode 1. The governing equations of motion are given by

$$\begin{Bmatrix} \ddot{x}_1 \\ \ddot{x}_2 \end{Bmatrix} + \lambda\begin{bmatrix} 3 & -1 \\ -1 & 2 \end{bmatrix}\begin{Bmatrix} \dot{x}_1 \\ \dot{x}_2 \end{Bmatrix} + \begin{bmatrix} 2 & -1 \\ -1 & 1 \end{bmatrix}\begin{Bmatrix} x_1 \\ x_2 \end{Bmatrix} = -\begin{Bmatrix} \lambda_{NES}(\dot{x}_1 - \dot{y}) + C(x_1 - y)^3 \\ 0 \end{Bmatrix}$$
$$0.05\ddot{y} + \lambda_{NES}(\dot{y} - \dot{x}_1) + C(y - x_1)^3 = 0 \tag{12}$$

with parameters $\lambda = 0.004469$, $\lambda_{NES} = 4\lambda$, and $C = 1$. We assume that at time $t = 0+$ we apply the energy input $E_1(0) = 1$ to mode 1 through an impulsive excitation with the appropriate magnitude and spatial distribution, and we depict the corresponding transient modal responses in Fig. 7. We note that due to the essential nonlinearity of the NES, the (not directly excited) higher mode 2 engages in nonlinear interaction with the directly excited mode 1. This is evidenced by the beat phenomenon in the velocity time series of mode 2 [Fig. 7(*d*)], as well as in the high *negative* values of the instantaneous effective damping measure $\lambda_{2eff}(t)$ in the highly energetic initial phase of the response, and indicates that energy flows into that mode from the first linear mode and/or the NES. In the absence of an NES, the two (distinct) linear modes are uncoupled, so we conclude that the transfer of energy to the higher mode is provided by nonlinear modal coupling due to the essential nonlinearity of the NES.

This result demonstrates that the instantaneous effective damping measures are capable of capturing positive or negative energy flows in structural modes caused by nonlinear modal interactions induced by the essential nonlinearities of the attached NESs. The capacity of the NESs to not only absorb and locally dissipate energy from all structural modes but also redistribute energy within the structural modes (e.g., transferring energy from lower to higher frequencies) can be used effectively for passive mitigation designs of blast induced structural vibrations based on the modification of the structure by intentional strong nonlinearities. In the next section we employ the defined local and global effective measures in order to assess the enhancement in the stiffness and damping of the structural dynamics of a two-DOFs linear system with different types of NESs attached to it.

3 Parametric Studies of Effective Stiffness and Damping for Type-I, -II, and -III NESs

In all applications presented in this section, we consider the same two-DOFs (two-floor) linear system with different configurations of NESs forced by an impulsive excitation.

$$\begin{Bmatrix} \ddot{x}_1 \\ \ddot{x}_2 \end{Bmatrix} + \lambda\begin{bmatrix} 3 & -1 \\ -1 & 2 \end{bmatrix}\begin{Bmatrix} \dot{x}_1 \\ \dot{x}_2 \end{Bmatrix} + \begin{bmatrix} 2 & -1 \\ -1 & 1 \end{bmatrix}\begin{Bmatrix} x_1 \\ x_2 \end{Bmatrix} = \tilde{\underline{f}}_{NES}(x_1,x_2,\underline{y})$$
$$\underline{M}_{NES}\ddot{\underline{y}} + \underline{P}_{NES}(\underline{y},\dot{\underline{y}}) = -\underline{f}_{NES}(x_1,x_2,\underline{y})$$
$$\begin{Bmatrix} x_1(0) \\ x_2(0) \end{Bmatrix} = \begin{Bmatrix} 0 \\ 0 \end{Bmatrix}, \quad \begin{Bmatrix} \dot{x}_1(0) \\ \dot{x}_2(0) \end{Bmatrix} = \begin{Bmatrix} 2F \\ F \end{Bmatrix}, \quad \underline{y}(0) = 0, \quad \dot{\underline{y}}(0) = 0 \tag{13}$$

These initial conditions correspond to impulsive excitations $2F\delta(t)$ and $F\delta(t)$ applied to the first and second floors, respectively, with the system being initially at rest at $t = 0-$. In all cases considered, the attached NESs have a mass equal to 5% of the mass (floor) of the structures to which they are attached.

The first application concerns a type-I NES attached to the first floor of the system and governed by the equation of motion (12) and the parameters $\lambda = 0.004469$, $\lambda_{NES} = 4\lambda$, and $C = 1$. In Fig. 8 we depict the global effective measures for varying energy input into the system. We note a small increase in the effective stiffness for both modes that, depending on the level of input energy, can reach up to 7% for mode 2. A much more substantial increase in the effective damping measures is found, however, which can reach as high as 2.5 times the modal damping for mode 1 and 8 times for mode 2. However, the energy ranges of increased effective measures are rather narrow and differ for the two modes. Clearly, these results are unoptimized and are provided here to demonstrate the application of the effective measures; even for these unoptimized results, however, we show later that we can get significant improvement when we consider type-III NESs instead.

In Fig. 9 we present the instantaneous effective measures for a specific damped transition at initial energy $E(0) = 0.4$,

Downloaded 09 Jan 2012 to 18.7.29.240. Redistribution subject to ASME license or copyright; see http://www.asme.org/terms/Terms_Use.cfm

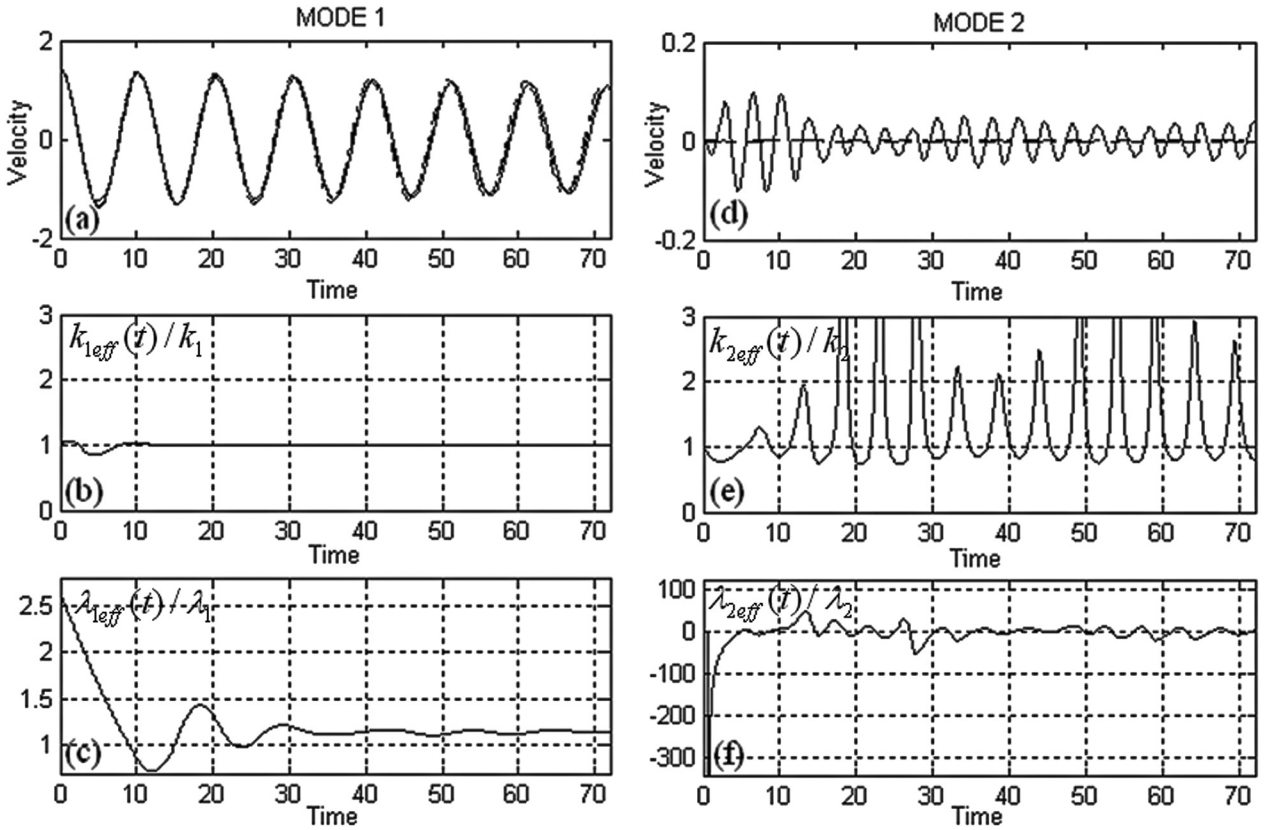

Fig. 7 Transient response of system (12) for impulsive excitation of the lowest linear mode 1. (*a*),(*d*) Velocity time series, (*b*),(*e*) normalized instantaneous effective stiffness, and (*c*),(*f*) normalized effective damping measure of modes 1 and 2, respectively; k_i and λ_i denote the modal stiffness and damping, respectively, of mode *i*.

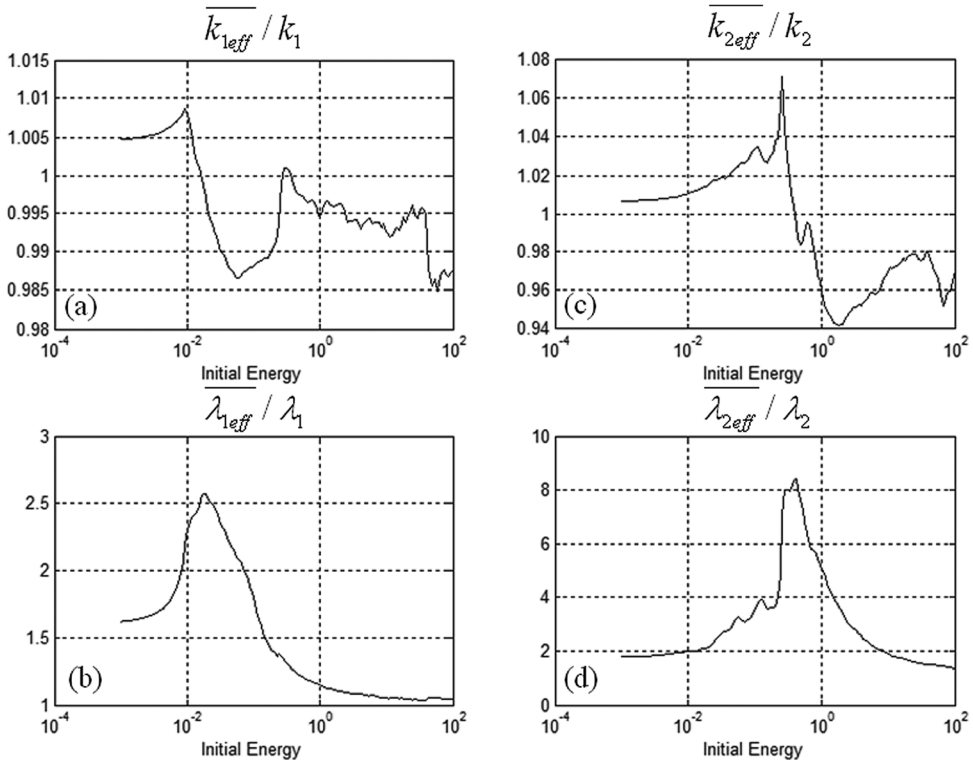

Fig. 8 Weighted-averaged (global) effective measures for the case of a single type-I NES attached to the first floor. Stiffness and damping measures for (*a*),(*b*) mode 1 and (*c*),(*d*) mode 2; k_i and λ_i denote the modal stiffness and damping, respectively, of mode *i*.

Downloaded 09 Jan 2012 to 18.7.29.240. Redistribution subject to ASME license or copyright; see http://www.asme.org/terms/Terms_Use.cfm

corresponding to weighted-averaged effective damping $\overline{\lambda_{2eff}}/\lambda_2 = 8.54$ for mode 2. In this case the second mode is damped very effectively, in contrast to mode 1, which has the weighted-averaged effective damping measure $\overline{\lambda_{1eff}}/\lambda_1 = 1.21$. The normalization constants $\lambda_i, i = 1,2$ refer to the modal constants of the two modes (under the assumption of proportional viscous damping). An interesting feature of these results is that there are time intervals in which the effective damping for mode 2 attains negative values; indeed, in these time intervals there occur beat phenomena (induced by the essential nonlinearity of the NES) as evidenced by the study of the percentages of instantaneous modal energies in Figs. 9(*d*) and 9(*h*). This result further confirms that the defined instantaneous (local) effective measures are capable not only of describing the efficacy of the NES in absorbing and dissipating modal energies, but also of capturing the energy transactions between modes caused by the intentional strong nonlinearity introduced in the system.

We now consider the case of a type-II NES (combining both nonlinear stiffness and damping) attached to the second floor of the two-DOFs system. In Ref. [16] it is shown that geometric nonlinear damping of the type incorporated in the type-II NES can give rise to interesting transient instability phenomena in the dynamics of the system to which it is attached. It follows that the introduction of essentially nonlinear damping into the system has the potential to generate new nonlinear dynamical phenomena, so its effect is not parasitic (as in the case of weak linear viscous damping). For this second application, the equations of motion governing the dynamics of the NES in Eq. (13) assume the form

$$\tilde{f}_{NES}(x_1, x_2, y) = -\left\{ \begin{array}{c} 0 \\ \lambda_{NES,NL}(\dot{x}_2 - \dot{y})(x_2 - y)^2 + C(x_2 - y)^3 \end{array} \right\}$$
$$0.05\ddot{y} + \lambda_{NES,NL}(\dot{y} - \dot{x}_2)(y - x_2)^2 + C(y - x_2)^3 = 0 \qquad (14)$$

with parameters $\lambda = 0.004469$, $\lambda_{NES,NL} = 10\lambda$, and $C = 1$. In Fig. 10 we present the weighted-averaged effective measures for this system. Again, there is an enhancement of the dissipative capacity of the system, as evidenced by the significant increase of the effective dissipative measures of both modes over broader energy intervals as compared to the previous case. Similar to the previous application, however, no significant enhancement of the stiffness measures is noted over the same energy intervals.

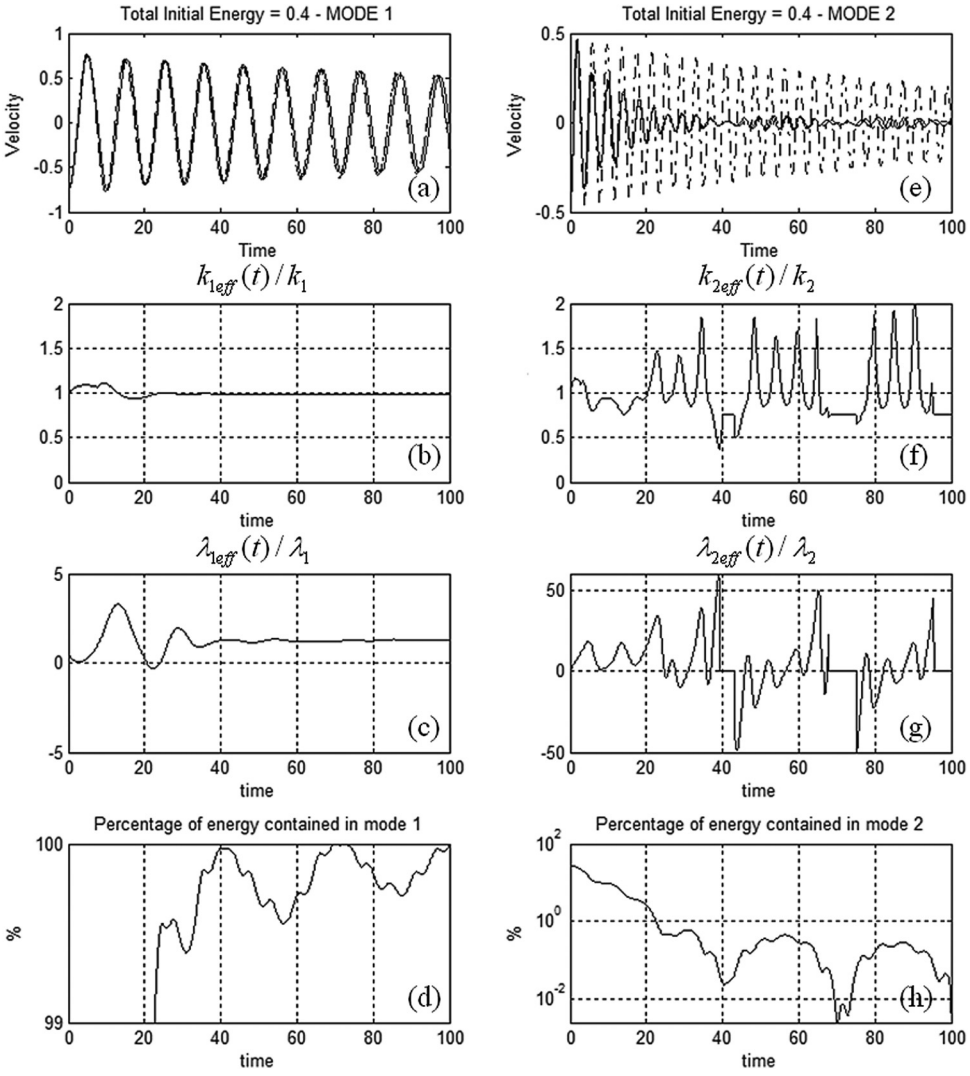

Fig. 9 Transient response of system (12) for impulsive excitation of impulse excitation with initial energy $E(0) = 0.4$. (*a*),(*e*) Velocity time series, (*b*),(*f*) normalized instantaneous effective stiffness, (*c*),(*g*) normalized effective damping measure, and (*d*),(*h*) percentage of instantaneous total energy of modes 1 and 2, respectively; k_i and λ_i denote the modal stiffness and damping, respectively, of mode *i*.

Downloaded 09 Jan 2012 to 18.7.29.240. Redistribution subject to ASME license or copyright; see http://www.asme.org/terms/Terms_Use.cfm

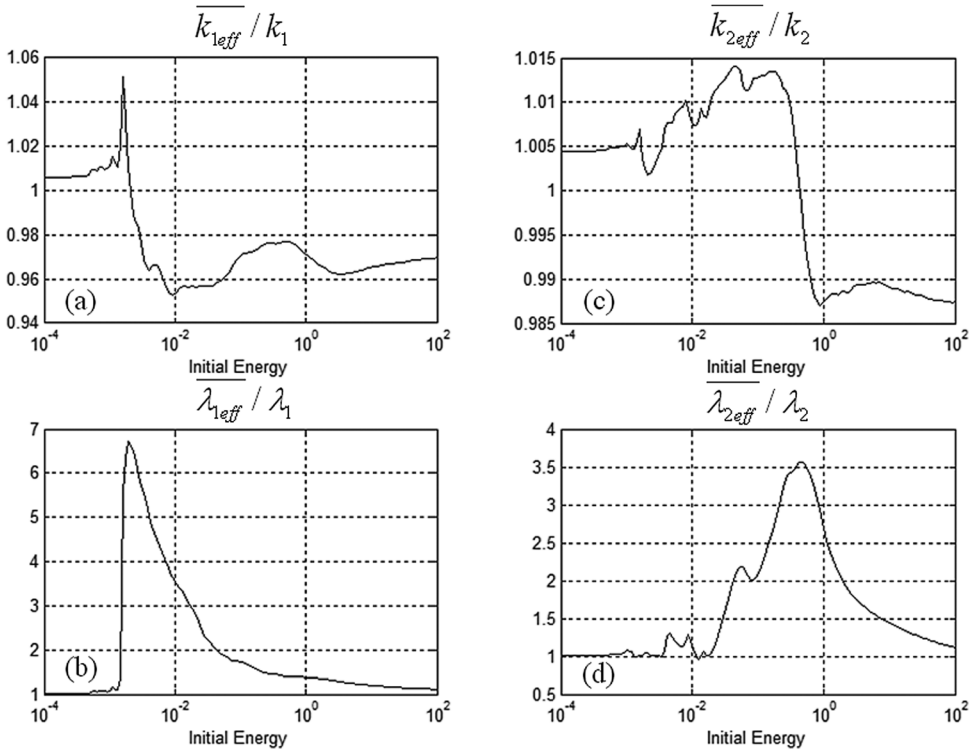

Fig. 10 Weighted-averaged (global) effective measures for the case of a single type-II NES attached to the second floor. Stiffness and damping measures for (*a*),(*b*) mode 1 and (*c*),(*d*) mode 2; k_i and λ_i denote the modal stiffness and damping, respectively, of mode *i*.

In an attempt to broaden the energy intervals of enhanced damping performance, in our third application we consider the addition of two identical type-III NESs, one to each of the two floors of the linear system [Figure 11(*a*)]. The equations governing the dynamics of the two NESs are then given by

$$\tilde{f}_{NES}(x_1,x_2,\underline{y}) = -\left\{\begin{array}{l}\lambda_{NES}(\dot{x}_1-\dot{y}_1)+C_1(x_1-y_1)^3\\ \lambda_{NES}(\dot{x}_2-\dot{y}_3)+C_2(x_2-y_3)^3\end{array}\right\}$$

$$0.025\ddot{y}_1+\lambda_{NES}(2\dot{y}_1-\dot{y}_2-\dot{x}_1)+C_1(y_1-x_1)^3+\sigma C_1(y_1-y_2)^3=0$$

$$0.025\ddot{y}_2+\lambda_{NES}(\dot{y}_2-\dot{y}_1)+\sigma C_1(y_2-y_1)^3=0$$

$$0.025\ddot{y}_3+\lambda_{NES}(2\dot{y}_3-\dot{y}_4-\dot{x}_2)+C_2(y_3-x_2)^3+\sigma C_2(y_3-y_4)^3=0$$

$$0.025\ddot{y}_4+\lambda_{NES}(\dot{y}_4-\dot{y}_3)+\sigma C_2(y_4-y_3)^3=0 \qquad (15)$$

with parameters $\lambda=0.004469, \lambda_{NES}=\rho\lambda, C_1=4, C_2=0.04$, and $\sigma=0.01$. We note that the total mass of each type-III NES is 5% of the mass of the floor to which it is attached, so no added mass effect is anticipated compared with the previous two applications. In addition, the two NESs are highly asymmetric; this is indicated by the small parameter σ that scales the two essential stiffness nonlinearities in each NES. The introduction of such high asymmetry is motivated by previous studies [9,18,21] in which it was shown that highly asymmetric multi-DOF NESs are very effective broadband passive absorbers of vibration energy, with the stiffer parts enabling the realization of strong resonance captures and the softer parts being effective dissipaters of vibration energy flowing in the NESs due to targeted energy transfer [9].

In Fig. 11 we depict the weighted-averaged effective measures for this system for three different values of the parameter ρ scaling the damping of the NESs. We note that an increase in the damping of the NESs does not necessarily lead to an enhancement of the effective modal damping measures; an optimization study is called for in order to design the NESs for efficient shock mitigation over defined energy ranges of interest. Considering the results of Fig. 11, we conclude that, in general, the addition of type-III NESs broadens the energy ranges of effective damping enhancement, but again no significant improvement in the stiffness is noted. Moreover, in contrast to the previous two applications, in which single-DOF NESs were considered, in this case there are two distinct energy ranges of increased effective damping measures, so it is possible to achieve increased effective damping measures for both modes over the same energy intervals. Typically, increasing the damping of the NESs increases the energy ranges of significant effective modal damping measures but decreases the peaks of the optimal increase of these measures.

In order to illustrate the broadband nature of the passive absorption of energy by the NESs, in Fig. 12 we study a specific damped transition corresponding to $\rho=1$ and an initial energy $E(0)=1.2$ corresponding to the weighted-averaged effective measures $\overline{\lambda_{1eff}}/\lambda_1=3.06$, $\overline{k_{1eff}}/k_1=0.97$, $\overline{\lambda_{2eff}}/\lambda_2=3.44$, and $\overline{k_{2eff}}/k_2=1.02$, where k_i and λ_i are normalization constants referring to the *i*th modal stiffness and damping, respectively. In Figs. 12(*c*) and 12(*d*) we depict the wavelet spectra of the relative responses between the first floor and the left mass of the NES attached to it, and between the two masses of the same NES, respectively. In Figs. 12(*e*) and 12(*f*) we provide the corresponding wavelet spectra for the upper floor and the NES attached to it. Wavelet transform spectra provide us with the temporal evolution of the basic harmonic components of the transient nonlinear responses, in contrast to the classical Fourier transform, which provides only a "static" description of the harmonic content of the time series. As discussed and demonstrated in numerous applications in Ref. [9], the wavelet transform is a powerful signal processing method for analyzing the transient dynamics of strongly nonlinear systems, so it represents a very useful tool for studying the dynamics of highly complex, strongly nonlinear dynamical systems such as the ones considered herein. The wavelet spectra of Figs. 12(*c*) and 12(*d*) illustrate clearly that the NES attached to the first floor engages in high-frequency broadband resonance interaction with the linear structure, absorbing energy by exciting

Downloaded 09 Jan 2012 to 18.7.29.240. Redistribution subject to ASME license or copyright; see http://www.asme.org/terms/Terms_Use.cfm

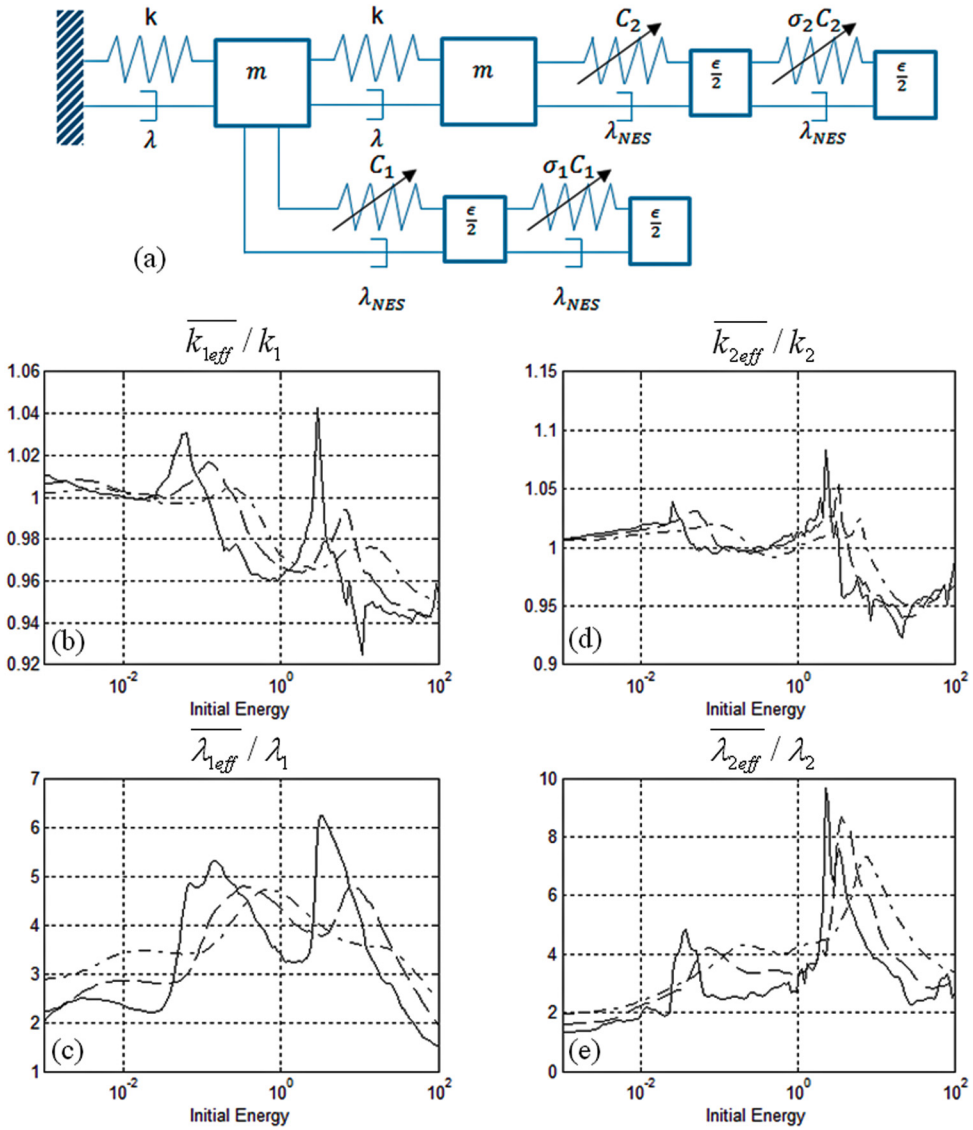

Fig. 11 Weighted-averaged (global) effective measures for the case of two type-III NESs attached to the first and second floors. (*a*) Configuration of the system. Stiffness and damping measures for (*b*),(*c*) mode 1 and (*d*),(*e*) mode 2; k_i and λ_i denote the modal stiffness and damping, respectively, of mode *i*; -·-·-·- $\rho = 4$, - - - - $\rho = 2$, —— $\rho = 1$.

high-frequency modes above the linear modes of the structure. As discussed in Ref. [9], such modes are essentially nonlinear (i.e., they have no counterparts in linear theory) and are induced in the augmented structure by the strong intentional nonlinearities of the NESs. Additional lower frequency modes exist as well, as evidenced by the excitation shown in Fig. 12(*d*) of an intermediate-frequency nonlinear mode between the two linear structural modes. The introduction and excitation of strongly nonlinear modes in the augmented structure is one of the possible dynamical mechanisms through which the NESs passively absorb and redistribute (scatter) shock energy with the linear structure. No such broadband energy absorption and scattering is noted in the wavelet spectra of Figs. 12(*e*) and 12(*f*), indicating that the upper-level NES resonantly interacts with the linear structural modes, as well as with a strongly nonlinear mode lying between the structural modes.

4 Concluding Remarks

The results reported in this work demonstrate that the use of intentional strong stiffness and/or damping nonlinearities can enhance the effective damping properties of a linear structure. The implementation of strong nonlinearity was achieved through the use of local NESs with the capacity to affect the global dynamics of the structure to which they are attached. This is made possible by the essential (nonlinearizable) dynamics of the NESs and the complete lack of linear components in their dynamics, which enables them to engage in resonance capture with single or multiple structural modes over broad frequency and energy ranges. In turn, such resonance interactions lead to targeted energy transfer from structural modes to the NESs and to the possibility of a redistribution of nonlinear vibration energy within the structural modes. In particular, the possibility of low- to high-energy energy transfer between structural modes offers an interesting new way of reducing and dissipating shock-induced energy in a structure, resulting in effective passive shock mitigation designs.

Single or multi-DOF NESs can increase drastically the effective modal damping of a linear structure, although their effective stiffening effects are less profound. Clearly, optimization studies are needed in order to design essentially nonlinear attachments that lead to stiffness and damping enhancement over broad energy ranges for shock inputs of varied frequency content. In particular,

Downloaded 09 Jan 2012 to 18.7.29.240. Redistribution subject to ASME license or copyright; see http://www.asme.org/terms/Terms_Use.cfm

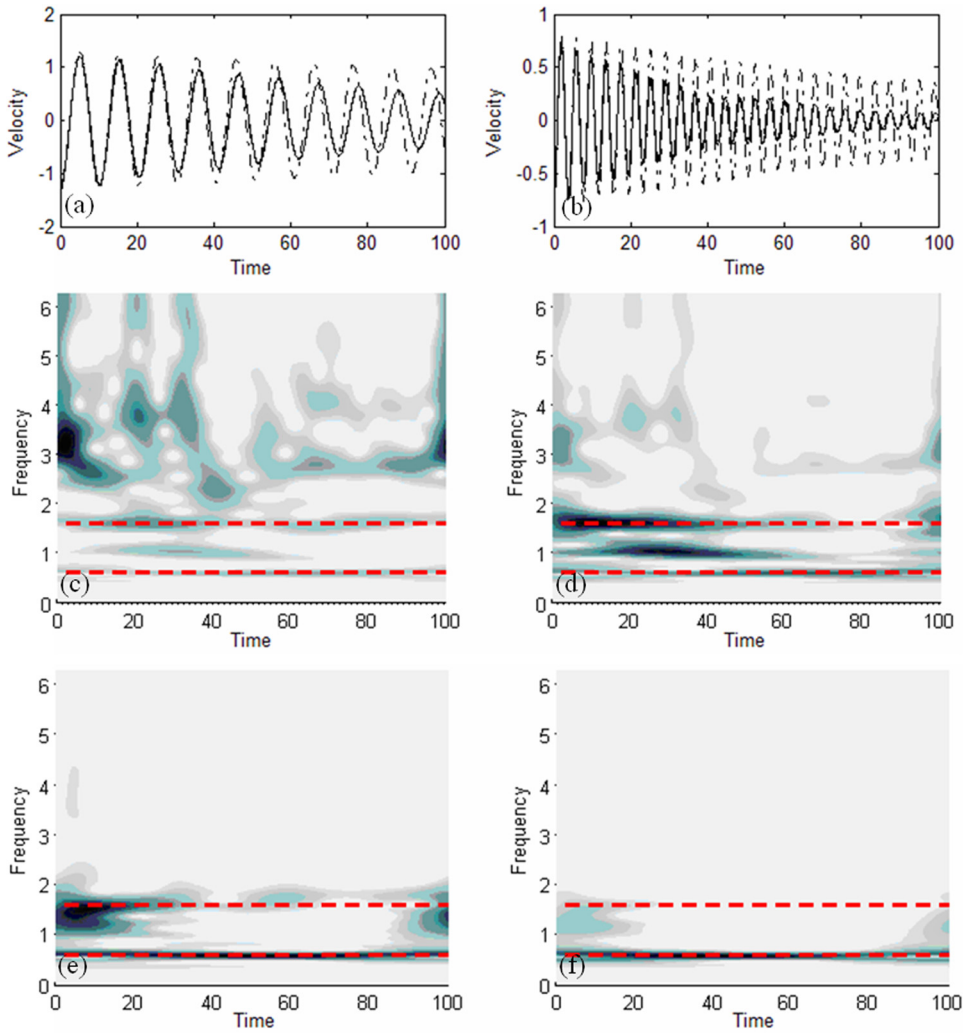

Fig. 12 Damped transition of the system with two type-III NESs for initial energy $E(0) = 1.2$. Velocity time series of (*a*) mode 1 and (*b*) mode 2. Wavelet transform spectra of (*c*) $x_1 - y_1$, (*d*) $y_1 - y_2$, (*e*) $x_2 - y_3$, and (*f*) $y_3 - y_4$; dashed lines indicate the natural frequencies of the linear structure.

the capacity of the multi-DOF type-III NES to engage in broadband dynamical interaction with structural modes offers encouraging progress toward that goal.

The strongly nonlinear system considered here involves two fundamental assumptions. First, the nonlinear stiffness elements did not possess any linear stiffness components. As discussed in Vakakis et al. (2008), a small linear component would not qualitatively affect the response, introducing only a small perturbation to the derived results and not restricting the practical results of the analysis. Another important assumption is the absence of other sources of dissipation, such as dry friction effects. In current practical implementations of the proposed designs, special attention is given to reducing the dry friction effects as much as possible, because these unmodeled forces would affect the nonlinear dynamics. Future work will demonstrate the practical implementation of the proposed designs to reliably reproduce the theoretically predicted results. We conclude by emphasizing that the effective measures of stiffening and damping introduced in this work are able to capture the effect of the essentially nonlinear attachment on the response of the structural system. In particular, these effective measures can be used to quantify the augmentation of damping, as well as the coupling that is introduced between the linear structural modes of the system.

Acknowledgment

This research program is sponsored by the Defense Advanced Research Projects Agency through grant HR0011-10-1-0077; Dr. Aaron Lazarus is the program manager. The content of this paper does not necessarily reflect the position or the policy of the government, and no official endorsement should be inferred.

References

[1] Nayfeh, A. H., and Mook D., 1990, *Nonlinear Oscillations*, Wiley, New York.
[2] Manevitch, L. I., 1999, "Complex Representation of Dynamics of Coupled Oscillators," in *Mathematical Models of Nonlinear Excitations, Transfer Dynamics and Control in Condensed Systems*, Kluwer Academic/Plenum, New York.
[3] Aboudi, J., 1993, "Response Prediction of Composites Composed of Stiffening Fibers and Nonlinear Resin Matrix," Compos. Sci. Technol., **46**, pp. 51–58.
[4] Karray, F., Grewal, A., Glaum, M., and Modi, V., 1997, "Stiffening Control of a Class of Nonlinear Affine Systems," IEEE Trans. Aerosp. Electron. Syst., **33**(2), pp. 473–484.
[5] Kasza, K. E., Nakamura, F., Hu, S., Kollmannsberger, P., Bonakdar, N., Fabry, B., Stossel, T. P., Wang, N., and Weitz, D. A., 2009, "Filamin A Is Essential for Active Cell Stiffening but Not Passive Stiffening Under External Force," Biophys. J., **96**, pp. 4326–4335.
[6] Lakes, R. S., 2001, "Extreme Damping in Composite Materials With a Negative Stiffness Phase," Phys. Rev. Lett., **86**(13), pp. 2897–2900.
[7] Wang, Y. C., and Lakes, R. S., 2003, "Extreme Stiffness Systems Due to Negative Stiffness Elements," Am. J. Phys., **72**(1), pp. 40–50.

Downloaded 09 Jan 2012 to 18.7.29.240. Redistribution subject to ASME license or copyright; see http://www.asme.org/terms/Terms_Use.cfm

[8] Huang, H. H., and Sun, C. T., 2009, "Wave Attenuation Mechanism in an Acoustic Metamaterial With Negative Effective Mass Density," New J. Phys., **11**, 013003.
[9] Vakakis, A. F., Gendelman, O., Bergman, L. A., McFarland, D. M., Kerschen, G., and Lee, Y. S., 2008, *Passive Nonlinear Targeted Energy Transfer in Mechanical and Structural Systems: I and II*, Springer, New York.
[10] Arnold, V. I., ed., 1988, *Encyclopedia of Mathematical Sciences, Dynamical Systems III*, Springer-Verlag, Berlin, 1988.
[11] Geldenman, O. V., Manevitch, L. I., Vakakis, A. F., and M'Closkey, R., 2001, "Energy Pumping in Nonlinear Mechanical Oscillators I: Dynamics of the Underlying Hamiltonian Systems," J. Appl. Mech., **68**(1), pp. 34–41.
[12] Vakakis, A. F., and Gendelman, O. V., 2001, "Energy Pumping in Nonlinear Mechanical Oscillators II: Resonance Capture," J. Appl. Mech., **68**, pp. 42–48.
[13] Vakakis, A. F., 2001, "Inducing Passive Nonlinear Energy Sinks in Vibrating Systems," J. Vibr. Acoust., **123**, pp. 324–332.
[14] Gourdon, E., Coutel, S., Lamarque, C. H., and Pernot, S., 2005, "Nonlinear Energy Pumping With Strongly Nonlinear Coupling: Identification of Resonance Captures in Numerical and Experimental Results," Proceedings of the 20th ASME Biennial Conference on Mechanical Vibration and Noise, Long Beach, CA, Sept. 24–28.
[15] McFarland, D. M., Bergman, L. A., and Vakakis, A. F., 2005, "Experimental Study of Nonlinear Energy Pumping Occurring at a Single Fast Frequency," Int. J. Non-Linear Mech., **40**, pp. 891–899.
[16] Andersen, D., Starosvetsky, Y., Vakakis, A. F., and Bergman, L. A., "Dynamic Instabilities in Coupled Oscillators Induced by Geometrically Nonlinear Viscous Damping," Nonlinear Dyn.
[17] Quinn, D. D., Triplett, A. L., Vakakis, A. F., and Bergman, L. A., "Energy Harvesting from Impulsive Loads Using Intentional Essential Nonlinearities," J. Vibr. Acoust., **133**, 011004.
[18] Gendelman, O. V., Sapsis, T., Vakakis, A. F., and Bergman, L. A., 2011, "Enhanced Passive Targeted Energy Transfer in Strongly Nonlinear Mechanical Oscillators," J. Sound Vib., **330**, pp. 1–8.
[19] Nucera, F., Lo Iacono, F., McFarland, D. M., Bergman, L. A., and Vakakis, A. F., 2008, "Application of Broadband Nonlinear Targeted Energy Transfers for Seismic Mitigation of a Shear Frame: Part II, Experimental Results," J. Sound Vib., **313**, pp. 57–76.
[20] Nucera, F., McFarland, D. M., Bergman, L. A., and Vakakis, A. F., 2010, "Application of Broadband Nonlinear Targeted Energy Transfers for Seismic Mitigation of a Shear Frame: Part I, Computational Results," J. Sound Vib., **329**(15), pp. 2973–2994.
[21] Tsakirtzis, S., Panagopoulos, P. N., Kerschen, G., Gendelman, O., Vakakis, A. F., and Bergman, L. A., 2007, "Complex Dynamics and Targeted Energy Transfer in Systems of Linear Oscillators Coupled to Multi-Degree-of-Freedom Essentially Nonlinear Attachments," Nonlinear Dyn., **48**, pp. 285–318.
[22] Xu, X., and Kup, Y., "Tensegrity Structures With Buckling Members Explain Nonlinear Stiffening and Reversible Softening of Actin Networks," J. Eng. Mech., **135**(12), pp. 1368–1374.

Downloaded 09 Jan 2012 to 18.7.29.240. Redistribution subject to ASME license or copyright; see http://www.asme.org/terms/Terms_Use.cfm